REPORT

EVALUATION OF HIGH DENSITY POLYETHYLENE DUCTS OF THE SUNSHINE SKYWAY BRIDGE

for

Florida State of Department of Transportation
State Materials Office
5007 Northeast 39th Avenue
Gainesville, Florida 32609

Submitted by

Dr. Y. Grace Hsuan
Civil, Architectural and Environmental Engineering
Drexel University
Philadelphia, PA 19104

August 12, 2004

Table of Contents

List of Tables

List of Figures

ABSTRACT

This study is focused on the evaluation of high-density polyethylene (HDPE) ducts in the Sunshine Skyway (SSK) Bridge. It is a part of research project entitled "Investigation of Stress Cracking of HDPE Ducts in Segmental Bridges." sponsored by the Florida Department of Transportation (FDOT). The principal investigator of the project is Dr. William Hartt, Florida Atlantic University, and Dr. Grace Hsuan, Drexel University, is the subcontractor.

The purpose of the study is to assess the material properties of HDPE ducts, particularly the stress cracking resistance (SCR) behavior of SSK Bridge. Duct samples were retrieved from both column and span parts of the bridge. Thirty-two samples were removed from various column sections, and four of them contained longitudinal cracks. Thirty-four samples were removed from five different span sections and three of them contained longitudinal cracks.

The cracking mechanism was identified to be slow crack growth based on the fracture morphology. The cracking of the column sample was initiated by impurities located at the inner surface of the duct. The crack initiation of the span sample could not be clearly identified; however, impurities were also observed in the material.

The material properties of the duct were evaluated according to tests specified by AASHTO specification. Two of the specified tests were not performed due to sample configuration and poor precision of the test. However, SP-NCTL test and OIT test are added to the evaluation. The majority of the field samples failed to conform to the required values of the melt-index and carbon black. In addition, the SP-NCTL tests exhibited failure times less than 10 hours, expect for two columns and one span samples. The OIT values of the field samples were less than 10 minutes.

The test results indicate large variability in the properties for both column and span ducts, particularly the column duct samples. For the span duct samples, some consistencies in the material properties can be observed in different sections of the bridge.

By comparing failure time of the SP-NCTL tests to density and MI, the MI gives a better correlation with failure time than the density. Although the relatively low molecular weight (high MI) and high crystallinity (high density) of the resins are contributing factors to the cracking, neither MI nor density can precisely predict the SCR of the material.

INTRODUCTION

This report presents the test results of high-density polyethylene (HDPE) duct samples that were retrieved from supporting columns and superstructure spans of the Sunshine Skyway (SSK) Bridge. The properties of the HDPE ducts, particularly the stress cracking resistance (SCR) were evaluated. For samples that contain cracks the cracking mechanism was investigated. The material properties were assessed using the ASTM D 3350 specification. In addition, the single point notched constant tensile load (SP-NCTL) test was utilized to determine the SCR while the oxidation induction time (OIT) test was used to assess the remaining antioxidants in the retrieved field samples.

TEST MATERIALS

Two groups of samples were evaluated in this study. One group was taken from supporting columns of the SSK Bridge and the other was from the superstructure span of the bridge.

Column Samples

Thirty-two samples were retrieved from different columns of the SSK Bridge, as shown in Table 1. Half of the samples were retrieved from southbound columns and the others from northbound columns. Four of the 32 samples each had a longitudinal crack. Two of the cracked ducts were taken from southbound columns and the other two from northbound columns. The thickness of each of 27 ducts was measured to determine the precision of the manufacturing. The material properties were evaluated on 14 of the 32 samples. The results of the tests are presented.

Span Samples

Thirty-four span samples were retrieved from the superstructure of the SSK Bridge. Table 2 shows the locations of retrieved samples with respect to different sections of the bridge. The number listed in Table 2 will be used for sample identification in data analyses. Three samples each had a longitudinal crack and they were all taken from the northbound north approach (NB-NA) span.

THICKNESS EVALUATION OF COLUMN SAMPLES

Of the 32 retrieved column duct samples, 27 of them were selected to assess the precision of the thickness. The thickness measurements were carried out by Mr. Florent David from Florida Atlantic University and sent to us for analyzing. The test procedure and analysis were performed according to ASTM D 2122. Eight individual thickness values were measured from each retrieved field sample. The

average wall thickness, S, and wall thickness range, E, are calculated. The wall thickness range, E, is expressed in percentage and is obtained using Equation (1).

Table 1 – Identification of the Thirty-two Retrieved Column Duct Samples

Sample No.	Duct Identification	Feature	Type of Test	
			Thickness	Material Property
Southbound				
C-1	91-SB-SW-5	Duct #1	X	X
C-2	91-SB-NE-5	Duct #2	X	X
	91-SB-NW-5	Duct #2	X	
C-3	103-SB-NW-12	Duct #2, Cut	X	X
	103-SB-NE-11	Duct #2	X	
	103-SB-NW-11	Duct #2	X	
	103-SB-NE-5	Duct #2	X	
	103-SB-NW-5	Duct #2	X	
C-4	118-SB-SE-6	Duct #1, Vertical Crack		X
	118-SB-NW-12	Duct #2	X	
	118-SB-NE-12	Duct #2	X	
C-5	118-SB-NW-6	Duct #2	X	X
	118-SB-NE-6	Duct #2	X	
C-6	131-SB-NE-5	Duct #2		X
	131-SB-SW-5	Duct #1	X	
C-7	131-SB-SE-6	Duct #1, Vertical Crack	X	X
Northbound				
C-8	92-NB-NE-5	Duct #2		X
C-9	92-NB-SW-5	Duct #1		X
	95-NB-SW-5	Duct #1	X	
	95-NB-SE-5	Duct #1	X	
C-10	95-NB-SE-8	Duct #1	X	X
	95-NB-SW-8	Duct #1	X	
	117-NB-NW-7	Duct #2	X	
C-11	117-NB-SW-7	Duct #1	X	X
	117-NB-NW-13	Duct #2	X	
	117-NB-SW-13	Duct #1	X	
C-12	117-NB-NW-8	Duct #2, Vertical Crack	X	X
C-13	119-NB-NW-11	Duct #2	X	X
	119-NB-NE-11	Duct #2	X	
	119-NB-NW-5	Duct #2	X	
	119-NB-NE-5	Duct #2	X	
C-14	119-NB-SE-12	Duct #1, Spiral Crack		X

Note:
Duct #1 was designated for the continuous duct coded SW-SE
Duct #2 was designated for the continuous duct coded NW-NE

Table 2 – Identification of the Thirty-four Retrieved Span Duct Samples

No.	Sample Identification	Duct Feature
Southbound-North Approach (SB-NA)		
S-1	134-SB T1-SEG7	No Crack
S-30	133-SB T2-SEG7-N	No Crack
S-2	126-SB T1-SEG7	No Crack
S-28	121-SB T2-SEG7-N	No Crack
S-29	121-SB T3-SEG7-N	No Crack
S-3	117-SB T1-SEG7	No Crack
S-27	117-SB T1-SEG6-N	No Crack
Southbound-South Approach (SB-SA)		
S-7	105-SB T1-SEG7	No Crack
S-8	96-SB T1-SEG7	No Crack
S-26	95-SB T2-SEG1-N	No Crack
S-9	88-SB T1-SEG7	No Crack
Northbound-North Approach (NB-NA)		
S-4	134-NB T1-SEG1	No Crack
S-5	126-NB T1-SEG1	No Crack
S-34	124-NB T3-SEG4-N	Cracked
S-33	119-NB T4-SEG1	Cracked
S-32	118-NB T3-SEG6-N	Cracked
S-6	117-NB T1-SEG1	No Crack
Northbound-South Approach (NB-SA)		
S-31	105-NB T6-SEG1-N	No Crack
S-10	105-NB T1-SEG1	No Crack
S-11	96-NB T1-SEG1	No Crack
S-12	88-NB T1-SEG1	No Crack
Main Stay		
S-13	116-T116-W325-SEG1	No Crack
S-14	115-T115-E-209-SEG19	No Crack
S-15	115-T116-W-408-SEG11	No Crack
S-16	113-T113-E-320-SEG17	No Crack
S-17	113-T113-E-405-SEG10	No Crack
S-18	112-STAY21-W-SEG21	No Crack
S-19	111-T111-W-302-SEG70	No Crack
S-20	110-STAY21-E-SEG21	No Crack
S-21	109-T109-W-320-SEG9	No Crack
S-22	187-T109-W-405-SEG18	No Crack
S-23	108-T108-W-208-SEG1	No Crack
S-24	107-T107-E-408-SEG10	No Crack
S-25	106-T106-E325-SEG5	No Crack

$$E = \frac{A - B}{A} \times 100 \quad (1)$$

where : A = maximum wall thickness at any cross section, and

B = minimum wall thickness at any cross section.

Table 3 shows the individual thickness value, minimum and maximum thickness values, average of the eight values and the thickness range of the eight values. The minimum wall thickness ranges from 0.131 to 0.176 inch, and the maximum thickness values are from 0.161 to 0.192 inches. The average wall thickness ranges from 0.153 inch to 0.180 inch, while the thickness range percentage varies from 3% to 32%.

Although the specification for the ducts was not available, the thickness tolerance should not exceed 0.020 inch for either inside or outside diameter controlled pipe. If the pipe was manufactured based on inside diameter controlled specification, the maximum permitted wall thickness should be the defined minimum thickness value plus 0.02 inch. In this case, the nominal pipe diameter is 2.5 inches and the SIDR is 15. According to ASTM D 2239, the minimum wall thickness is defined to be 0.165 inch; thus, the maximum thickness should be limited to 0.185. The majority of the pipes fails to pass the dimension specification.

EVALUATION OF CRACKING MECHANISM

The Cracking Mechanisms is investigated by examining the microstructure of the fracture surface using a scanning electron microscope (SEM). From the fraction morphology, the crack initiation and propagation direction can be identified, as well as cracking mechanism.

The microstructure of the cracked sample was evaluated by taking representative SEM specimens at different locations along the crack. One cracked column sample and one cracked span sample were examined.

Table 3 - Wall Thickness Information (unit in inch)

Sample	Duct Identification	Individual Thickness Value								Minimum Thickness	Maximum Thickness	Average Thickness	Thickness Range (%)
Southbound													
91-SB-NE-5	Duct #2	0.179	0.171	0.169	0.181	0.159	0.170	0.160	0.173	0.159	0.181	0.169	12%
91-SB-NW-5	Duct #2	0.180	0.189	0.169	0.180	0.192	0.177	0.169	0.184	0.169	0.192	0.180	12%
103-SB-NW-12	Duct #2	0.172	0.180	0.178	0.179	0.156	0.169	0.168	0.157	0.156	0.180	0.170	13%
103-SB-NE-11	Duct #2	0.187	0.176	0.170	0.168	0.170	0.173	0.176	0.184	0.168	0.187	0.176	10%
103-SB-NW-11	Duct #2	0.152	0.168	0.170	0.155	0.148	0.169	0.169	0.152	0.148	0.170	0.160	13%
103-SB-NE-5	Duct #2	0.180	0.172	0.163	0.161	0.160	0.160	0.174	0.172	0.160	0.180	0.168	11%
103-SB-NW-5	Duct #2	0.176	0.154	0.158	0.172	0.164	0.152	0.154	0.172	0.152	0.176	0.163	14%
118-SB-NW-12	Duct #2	0.161	0.161	0.172	0.150	0.172	0.168	0.164	0.166	0.150	0.172	0.164	13%
118-SB-NE-12	Duct #2	0.167	0.172	0.176	0.169	0.163	0.169	0.173	0.167	0.163	0.176	0.170	7%
118-SB-NW-6	Duct #2	0.174	0.189	0.178	0.170	0.177	0.184	0.191	0.168	0.168	0.191	0.179	12%
118-SB-NE-6	Duct #2	0.169	0.181	0.180	0.182	0.179	0.173	0.176	0.188	0.169	0.188	0.179	10%
131-SB-NE-5	Duct #2	0.174	0.188	0.150	0.174	0.175	0.165	0.151	0.162	0.150	0.188	0.167	20%
131-SB-SW-5	Duct #1	0.157	0.154	0.161	0.141	0.160	0.153	0.157	0.140	0.140	0.161	0.153	13%
131-SB-SE-6	Duct #1	0.156	0.151	0.183	0.168	0.168	0.172	0.179	0.169	0.151	0.183	0.168	17%
Northbound													
95-NB-SW-5	Duct #1	0.174	0.165	0.173	0.167	0.174	0.169	0.164	0.172	0.164	0.174	0.170	6%
95-NB-SE-5	Duct #1	0.172	0.167	0.150	0.174	0.163	0.170	0.158	0.158	0.150	0.174	0.164	14%
95-NB-SE-8	Duct #1	0.165	0.157	0.159	0.175	0.164	0.153	0.171	0.176	0.153	0.176	0.165	13%
95-NB-SW-8	Duct #1	0.183	0.171	0.168	0.177	0.170	0.171	0.161	0.177	0.161	0.183	0.172	12%
117-NB-NW-7	Duct #2	0.165	0.169	0.163	0.171	0.163	0.176	0.156	0.150	0.150	0.176	0.164	15%
117-NB-SW-7	Duct #1	0.176	0.178	0.181	0.182	0.178	0.182	0.178	0.177	0.176	0.182	0.179	3%
117-NB-NW-13	Duct #2	0.151	0.175	0.186	0.167	0.171	0.145	0.174	0.173	0.145	0.186	0.168	22%
117-NB-SW-13	Duct #1	0.174	0.153	0.179	0.175	0.178	0.158	0.148	0.180	0.148	0.180	0.168	18%
117-NB-NW-8	Duct #2	0.176	0.179	0.158	0.158	0.192	0.131	0.174	0.158	0.131	0.179	0.166	32%
119-NB-NW-11	Duct #2	0.175	0.182	0.178	0.172	0.173	0.170	0.176	0.170	0.170	0.182	0.175	7%
119-NB-NE-11	Duct #2	0.172	0.153	0.165	0.166	0.175	0.177	0.178	0.171	0.153	0.178	0.170	14%
119-NB-NW-5	Duct #2	0.168	0.171	0.165	0.168	0.170	0.165	0.170	0.169	0.165	0.171	0.168	4%
119-NB-NE-5	Duct #2	0.158	0.167	0.173	0.177	0.176	0.175	0.166	0.163	0.158	0.177	0.169	11%

- Column Sample 131-SB-SE-6

The sketch of the crack in the sample is shown in Figure 1. The length of the sample is approximately 34 inch long. The crack propagates longitudinally in a curved way. Two positions are marked as matching points. Three SEM specimens were taken from the crack and their approximately positions are indicated in Figure 1.

The general view of the fracture surface of Specimens 1 is shown in Figure 2. The fracture surface reveals a crack initiation as indicated by the hemisphere morphology. The initiation started from the inside surface of the duct and propagated through the thickness of the duct. The initiation seems to be caused by material defect on the inner surface of duct, as shown in Figure 3.

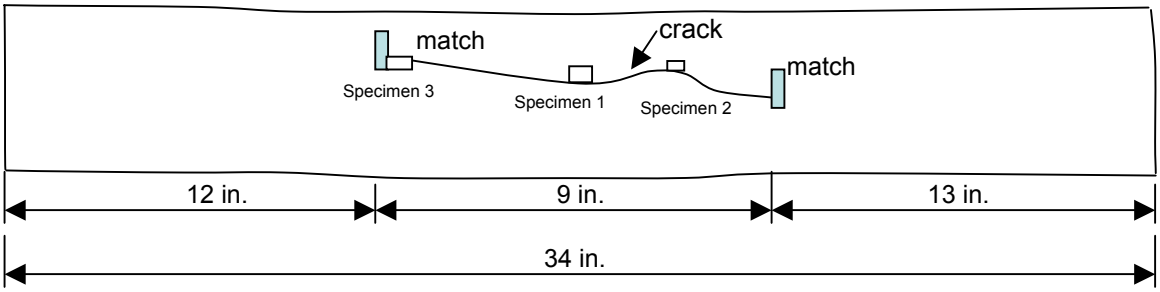

Figure 1 – Sketch of column Sample 131-SB-SE-6.

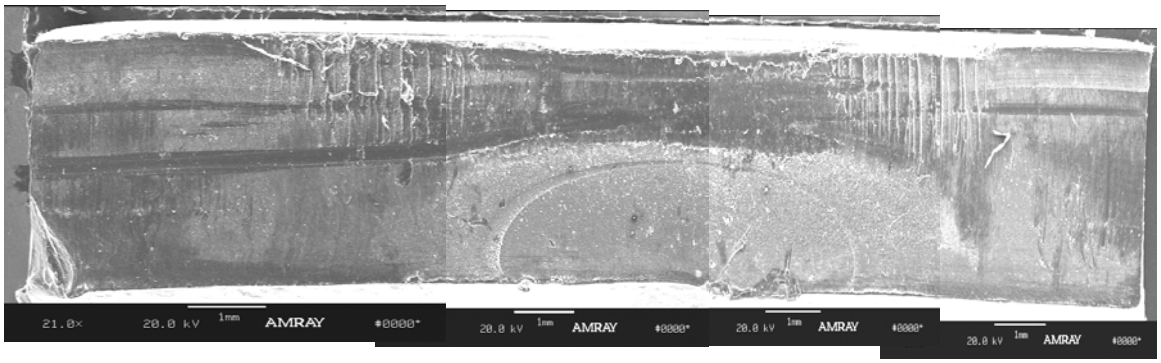

Figure 2 – Fracture surface of Specimen 1 from Sample 131-SB-SE-6

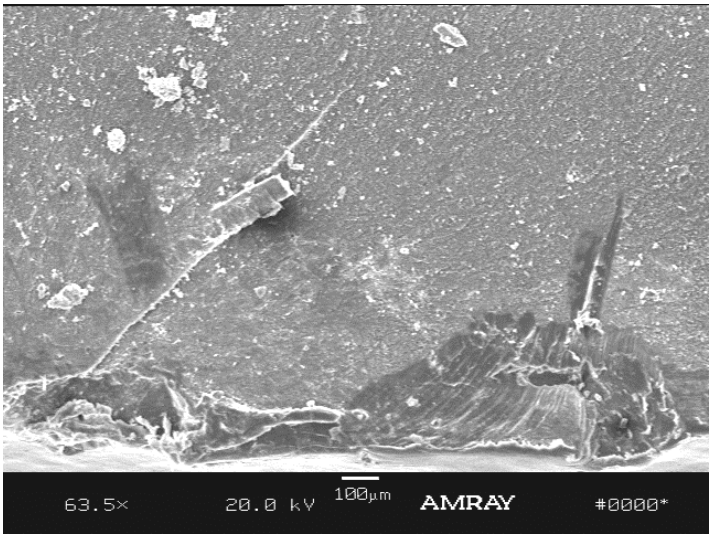

Figure 3 – A close view at the crack initiation point in Figure 2

The fracture surface of Specimen 1 is covered with short fibril structure, as can be seen in Figure 4. Such morphology is resulted from the slow crack growth via breaking down of fibers in the craze.

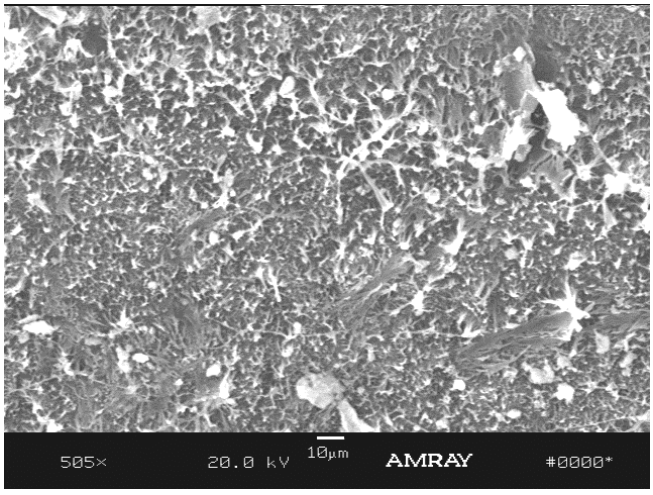

Figure 4 – Fracture morphology on the surface of Specimen 1

Specimen 2 was taken from some distance away from the crack initiation. The general view of the fracture surface is revealed in Figure 5. The area marked "A" in Figure 5 seems to be another crack initiation along this long crack. The close view of area "A" can be seen in Figure 6. The defect appears to be very similar to that in Figure 3.

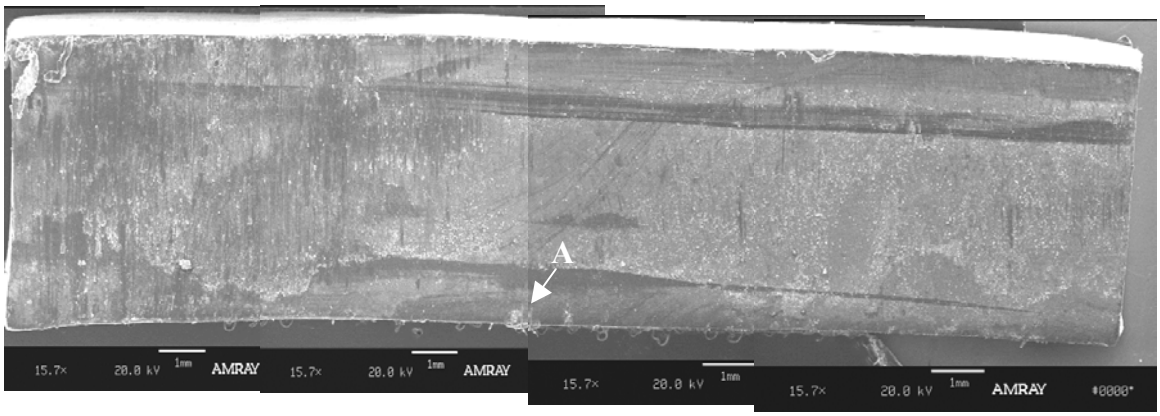

Figure 5 – General view of fracture surface of Specimen 2 from Sample 131-SB-SE-6

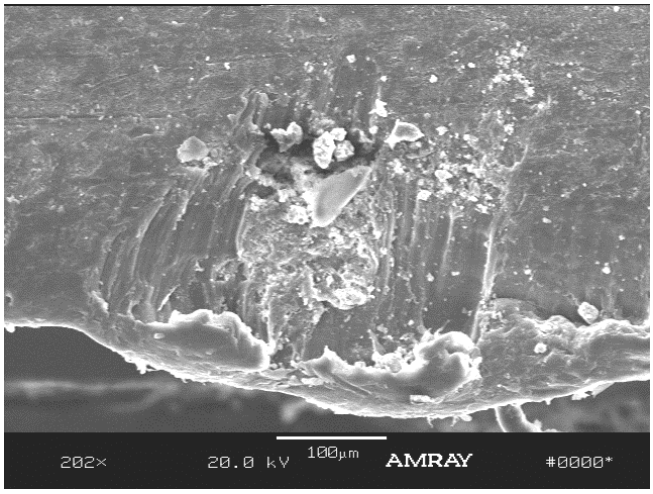

Figure 6 – A close view at area "A" of Figure 5

Specimen 3 was taken at the crack tip of the longitudinal crack. The general view of the fracture surface is revealed in Figure 7. The fracture surface of this specimen is covered with small fibril structure, as shown in Figure 8.

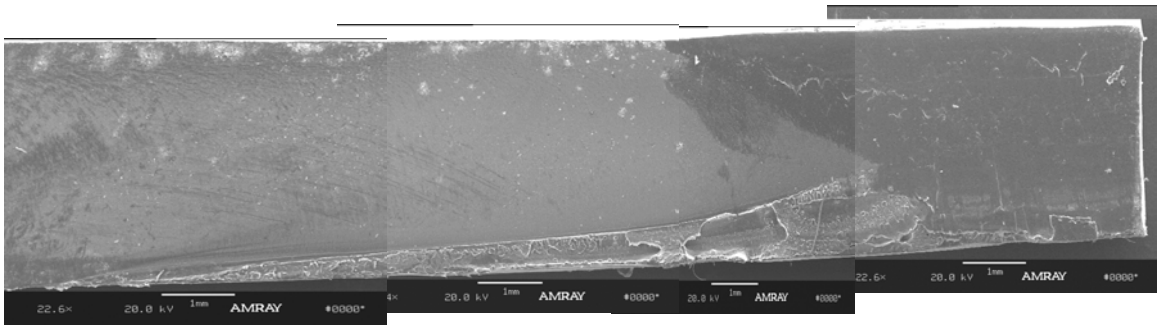

Figure 7 – General view of the fracture surface of Specimen 3 from Sample 131-SB-SE-6

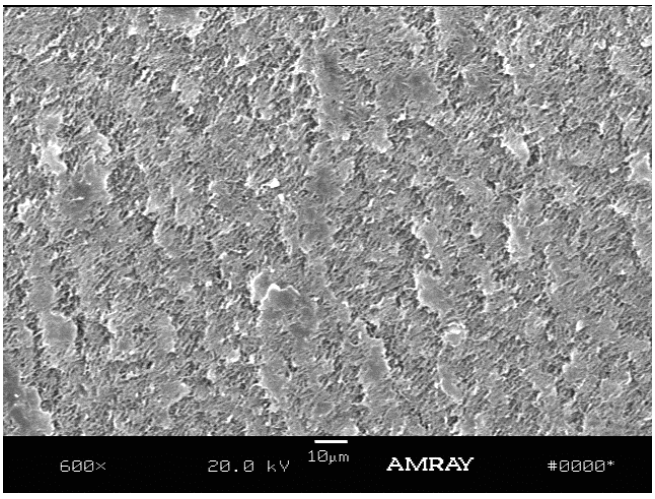

Figure 8 – The close view of fracture morphology of Specimen 3

- Span Sample 124NB-T3-SEG4-N

  The sample consists of a section of a long longitudinal crack. Under close exam of the fracture surface, there were no obvious features that indicated crack initiation in this section of the crack. Two SEM specimens were taken along the crack at some distance away from each other.

  Figure 9 reveals the fracture surface of Specimen 1. Two unique morphologies were observed on the fracture surface. One is in area "A" marked on Figure 9. A close view of area "A" is shown in Figure 10. It seems that there was an impurity imbedded in the material. The second morphology is marked in area "B". The close view of the area "B" can be seen in Figure 11. A series of parallel fatigue lines was observed, suggesting that cycling loading was involved in the crack growth.

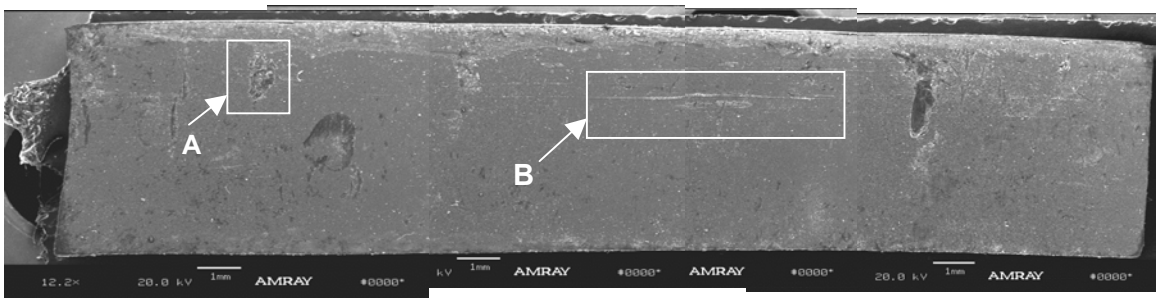

Figure 9 – General view of the fracture surface of Specimen 1 from Span Sample 124-NB-T3-SEG4-N

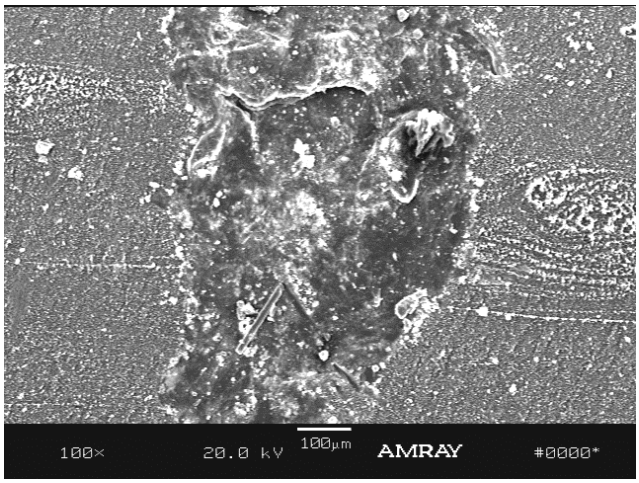

Figure 10 – A close view of area "A" of Figure 9 revealing impurity

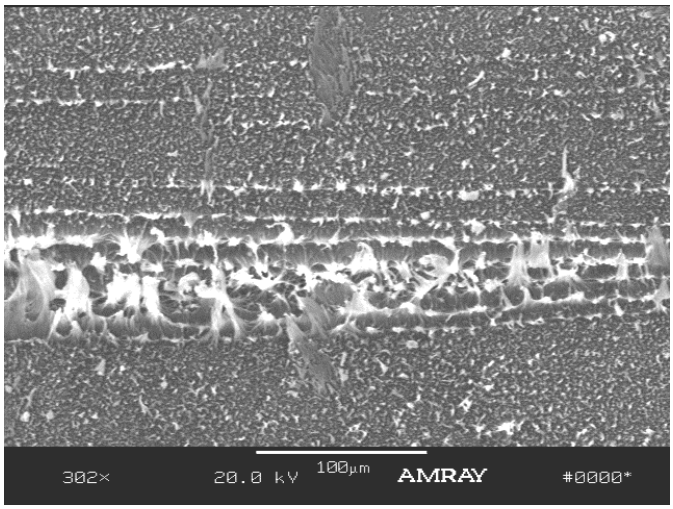

Figure 11 – A close view of area "B" of Figure 9, revealing fatigue lines

Figure 12 reveals the fracture surface of Specimen 2. Similar to Specimen 1, impurities and fatigue lines were also observed on this specimen, as shown in Figures 13 and 14, respectively. The fracture surfaces of both Specimens 1 and 2 were covered by small fibril structures, as shown in Figure 15. The cracking probably was caused by slow crack growth under periodical cycling loading.

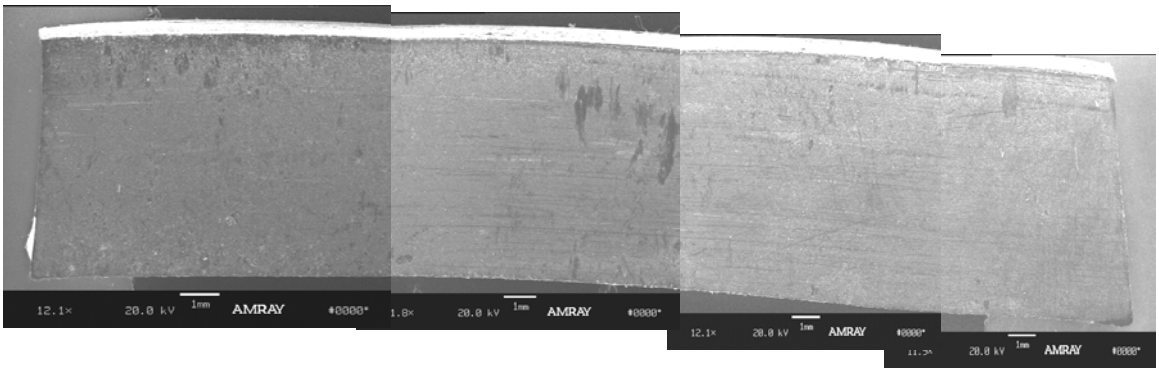

Figure 12 - General view of the fracture surface of Specimen 2 from Span Sample 124-NB-T3-SEG4-N

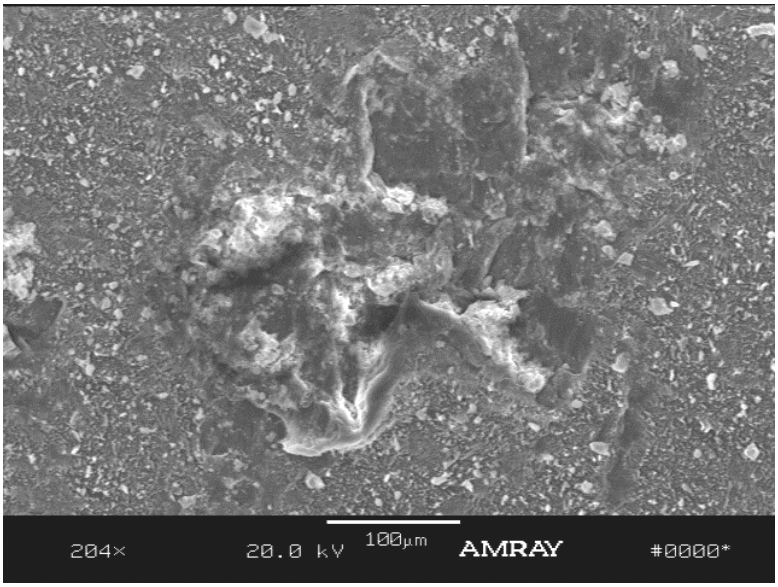

Figure 13 – Impurity observed on fracture surface of Specimen 2

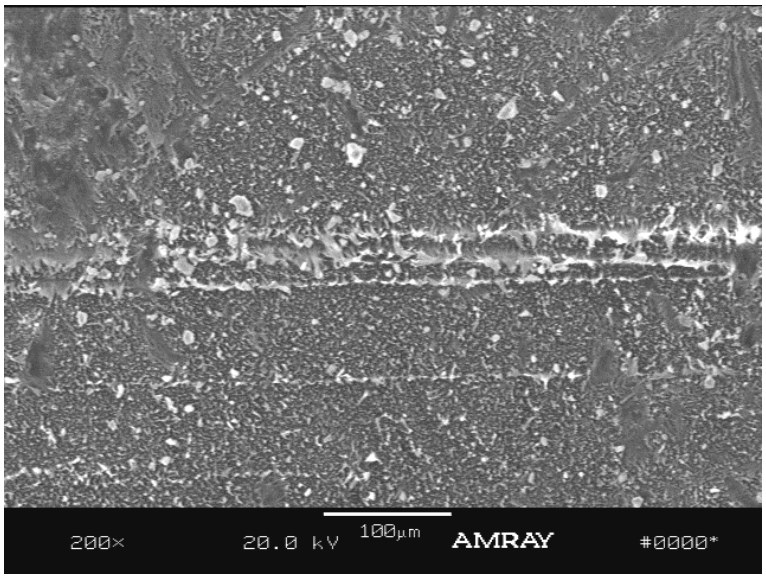

Figure 14 – Fatigue lines on the fracture surface of Specimen 2

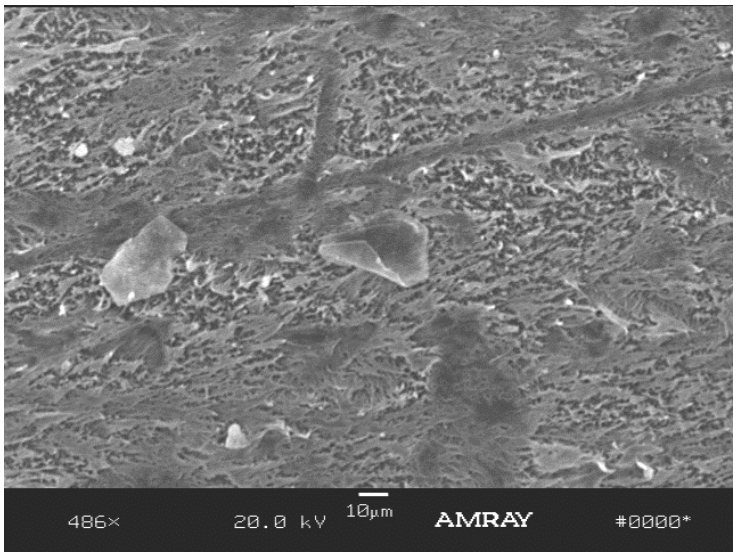

Figure 15 – Small fiber structure covered the fracture surfaces of Specimens 1 and 2

Discussion of Cracking Mechanisms

The fracture morphology provided preliminary information regarding the cracking mechanism of the cracked column and span samples. The microstructure indicates that cracking started from the inner surface of pipe wall and propagated through the wall thickness. The direction of the crack growth suggests that the inner duct surface was subjected to a tensile stress.

For column samples, crack initiations were found to take place at defects or impurities located on the inner surface of the duct. However, the crack initiation of the span sample could not be identified. The fatigue lines provided a good indication regarding the crack growth direction. Furthermore, some impurities were observed in the span sample; but they did not seem to act as the initiators of the crack. The cracking of both samples was governed by the slow crack growth mechanism.

MATERIAL PROPERTIES

Material properties of retrieved field ducts were evaluated largely based on test methods defined in the ASTM D 3350. The SCR property was measured using the SP-NCTL test (ASTM D5397-Appendix) using the AASHTO M 294 specification. In addition, the oxidative inductive time (OIT) test was included to assess the amount of antioxidant remaining in the polymer.

As indicated in Table 1, 14 of the 32 retrieved field samples were evaluated for their material properties. The four cracked ducts were included in the 14 samples. For span samples, nine field samples (Sample no. 26 to 34) were fully evaluated for their material properties. The other 25 samples were tested for their melt index and stress crack resistance.

According to Mr. Rodney Powers from Florida Department of Transportation (FL-DOT), the specification for this bridge merely stated to use HDPE ducts. However, the specific material requirements for the HDPE ducts were not defined. For comparison purpose, the material specification of smooth PE ducts from AASHTO (2000) is used as reference in this study. The AASHTO specification requires that "*Smooth plastic duct shall be made of polyethylene material and shall conform to the requirement of D 3350 with a cell classification PE 345433C*". Table 4 shows the required properties and corresponding values according to ASTM D 3350.

Table 4 - Specified Property for HDPE Duct According to ASTM Specifications

Property	Test Method	ASTM D 3350 Classification	Required Value
Density	ASTM D 1505	3	>0.940-0.955 (g/cc)
Melt index	ASTM D 1238	4	< 0.15 (g/10 min.)
Flexural Modulus	ASTM D 790	5	110,000 - <160,000 psi
Tensile yield strength	ASTM D 638 Type IV	4	3000 -<3500 psi
ESCR*	ASTM D 1693	3	F_{20} = 192 hr.
HDB**	ASTM D 2837	3	1250 psi
Carbon black	ASTM D 1603	C	> 2%
Additional Tests			
SP-NCTL[+]	AASHTO M294		> 24 hours
OIT	ASTM D3895		Not defined

* ESCR – environmental stress crack resistance
** HDB – hydrostatic design basis
\+ SP-NCTL – single point notched constant tensile load test
++ OIT – oxidative induction time

In this test program, material properties according to those listed in Table 4 were evaluated, but two tests were not included. One is the HDB test, which requires the test to be performed on uncracked pipe section; thus, the test is not applicable to retrieved field duct samples. The other test is the ESCR test, ASTM D 1693, which is a qualitative test to evaluate stress crack resistance (SCR) of HDPE materials. The test cannot quantitatively distinguish SCR among different materials and is known to have poor precision value. An alternative ESCR test is used in the study, and it is the SP-NCTL test according to ASTM 5397-appendix. The SP-NCTL test was recently adopted to replace the ASTM D 1693 test for corrugated HDPE non-pressured pipe in the AASHTO M294 specification. In addition, the OIT test is included to assess the amount of antioxidant remaining in the polymer. A short OIT value indicates a less amount of antioxidants for the same formulation. The result of this test can provide an indication on the level of antioxidant remaining in the duct samples.

Test Plaque Preparation.

All field duct samples were cleaned and cut into small pieces approximately one inch square in size. Compression molded plaques were prepared from these small pieces. The molding procedure followed ASTM D4703 Method B (at a cooling rate of 15 ± 5 ^{o}C/min). Three plaques with thickness of approximately 0.075 inches and one with a thickness of approximately 0.125 inches were made for each

duct sample. From these plaques, various test specimens were cut using appropriate dies and used for subsequent physical and mechanical testing to eventually be compared to the relevant project specification.

ASTM D3350 Specified Tests

The test procedure and results of each specified test are presented below:

- *Density* – The density test was performed according to ASTM D792 procedure B. The liquid used in the test was 1-Propanol with density of 0.781 g/cc at 23°C. The measurement was obtained using an analytical balance with an accuracy of 0.0001g. At least two replicates were evaluated for each sample. Note that the "true" resin density cannot directly be measured due to the added carbon black in the product; however, it can be calculated according to Equation 1. Tables 5 and 6 show the measured product density, carbon black content, and the calculated resin density for column and span samples, respectively.

$$\rho_{(resin)} = \rho_{(product)} - 0.0044C \qquad (1)$$

where: C = % carbon black in the product

The density values of column samples exhibit large variability with values ranging from 0.945 to 0.955 g/cc. Figure 16 shows the density values of 14 column samples in bar chart plot. All four cracked ducts, samples 4, 7, 12 and 14 have density equal or above 0.950 g/cc. Figure 17 shows the bar chart plot of density values of the nine span samples. Their densities are generally higher than those of the column samples. Except for one sample, all others have density value greater than 0.950 g/cc.

All retrieved field samples from both column and superstructure of the bridge conformed the resin density required range (0.940 – 0.955 g/cc) of cell class "3" in ASTM D3350.

Table 5 - Calculate the Density of the Resin and Carbon Black of Column Samples

No.	Sample Code	Product Density (g/cc)	Carbon Black (%)	Resin Density (g/cc)
Southbound				
C-1	91-SB-NE-5	0.949	0.50	0.947
C-2	91-SB-SW-5	0.958	0.90	0.954
C-3	103-SB-NW-12	0.956	0.30	0.955
C-4	118-SB-SE-6	0.956	1.00	0.952
C-5	118-SB-NW-6	0.954	1.60	0.947
C-6	131-SB-NE-5	0.960	1.90	0.952
C-7	131-SB-SE-6	0.961	2.10	0.952
Northbound				
C-8	92-NB-NE-5	0.958	0.40	0.956
C-9	92-NB-SW-5	0.955	0.30	0.954
C-10	95-NB-SE-8	0.947	0.20	0.946
C-11	117-NB-SW-7	0.952	1.70	0.945
C-12	117-NB-NW-8	0.956	1.00	0.952
C-13	119-NB-NW-11	0.948	0.60	0.945
C-14	119-NB-SE-12	0.954	0.80	0.950

Table 6 - Calculate the Density of the Resin and Carbon Black of Span Samples

No.	Sample Code	Density (g/cc)	Carbon Black (%)	Resin Density (g/cc)
Southbound				
S-26	95SB T2-SEG1-N	0.953	0.50	0.950
S-27	117SB T1-SEG6-N	0.952	0.60	0.949
S-28	121SB T2-SEG7-N	0.961	1.20	0.956
S-29	121SB T3-SEG7-N	0.954	0.45	0.952
S-30	133SB T2-SEG7-N	0.955	0.60	0.952
Northbound				
S-31	105NB-T6-SEG1-N	0.957	0.65	0.954
S-32	118NB-T3-SEG1-N	0.961	1.45	0.954
S-33	119NB-T4-SEG1	0.959	1.30	0.953
S-34	124NB-T3-SEG4-N	0.955	0.70	0.952

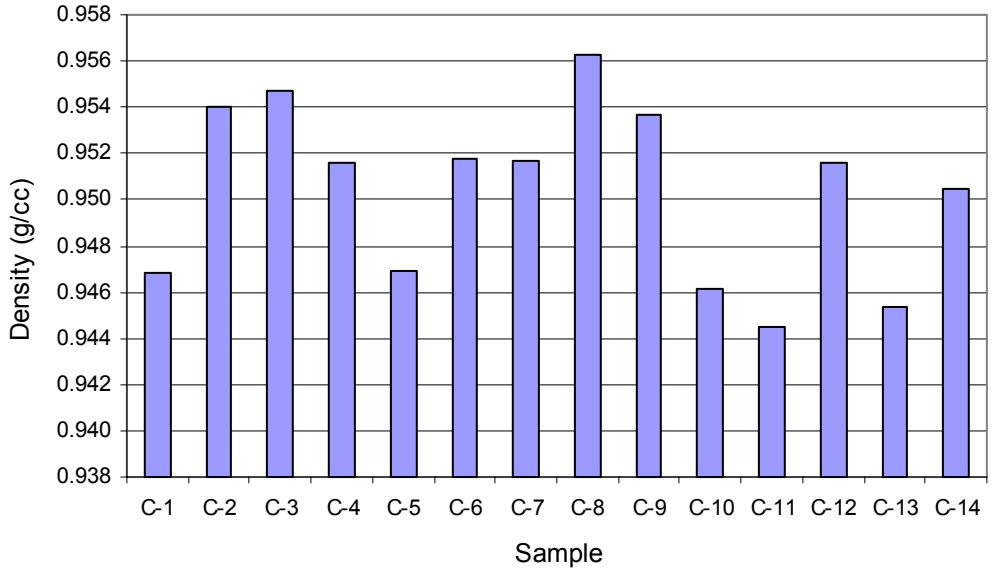

Figure 16 – Density variation of fourteen column samples

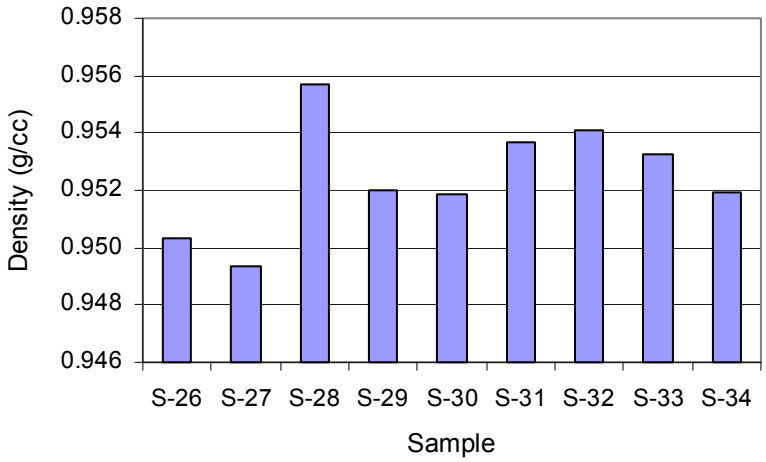

Figure 17 – Density variation of nine field span samples

- *Carbon Black* – The test to measure carbon black content was performed according to ASTM D 4812. Two replicates were evaluated for each sample. The test data are included in Tables 5 and 6 with the density for column and span samples, respectively.

  Except for one column sample, the carbon black content in both column and span samples are less than 2%, which is the minimum requirement as defined in the ASTM D3350. Furthermore, the range of carbon black content among different duct samples is very large, ranging from 0.3 to 2.1.

- *Melt index* – The melt index (MI) test was performed according to ASTM D1238 using a condition of 2.16 kg/190^{o}C. Two replicates were evaluated for each sample. The test results of 14 column samples are plotted in Figure 18 and the values are shown in Table 7. There is a large difference among 14 field samples. The MI value ranges from 0.09 to 0.91g/10 min. Samples 4, 7 and 12, which consist of a longitudinal crack, exhibit much higher MI values than the others. Sample 14 exhibits spiral cracking and has an average MI value.

  The MI values of 34 span samples are presented in Figure 19. The data are listed in Table 8. The samples are divided into five sections according to their locations in the bridge. The MI values vary significantly in each of the five sections, particularly the main stay (MS). In the NB-NA section, all six retrieved ducts samples have MI values greater than 0.4 g/10 min. In both NB-SA and SB-NA sections, the MI values of the retrieved duct samples can be divided into two groups: one with values around 0.2 g/10 min, and the other with values fall between 0.4 and 0.6 g/10 min. The ducts retrieved from the SB-SA section all have MI values less than 0.2 g/10 min. The greatest variation of MI is observed in the MS section, ranging from 0.1 to 1.1 g/10 min. The highest MI values belong to samples S-21, S-22, S-17 and S-16, which were taken from sections on either side of the central stay.

  All retrieved field samples from both the column and the spans of the bridge exhibited MI values well above the 0.15 g/10 min defined value based on cell classification of ASTM D3350.

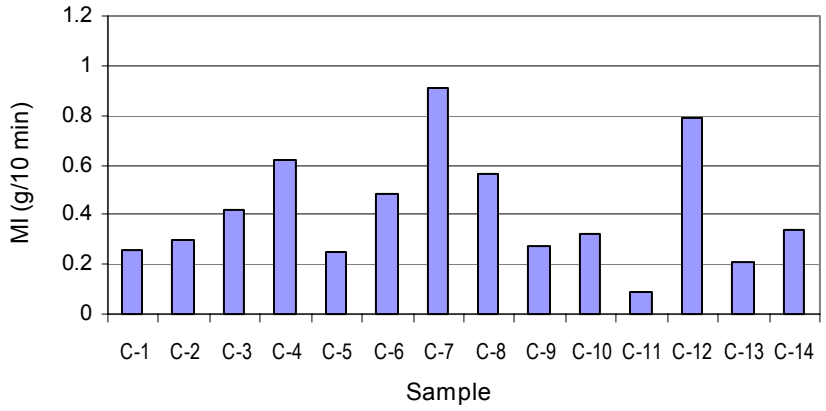

Figure 18 – MI values of fourteen column samples

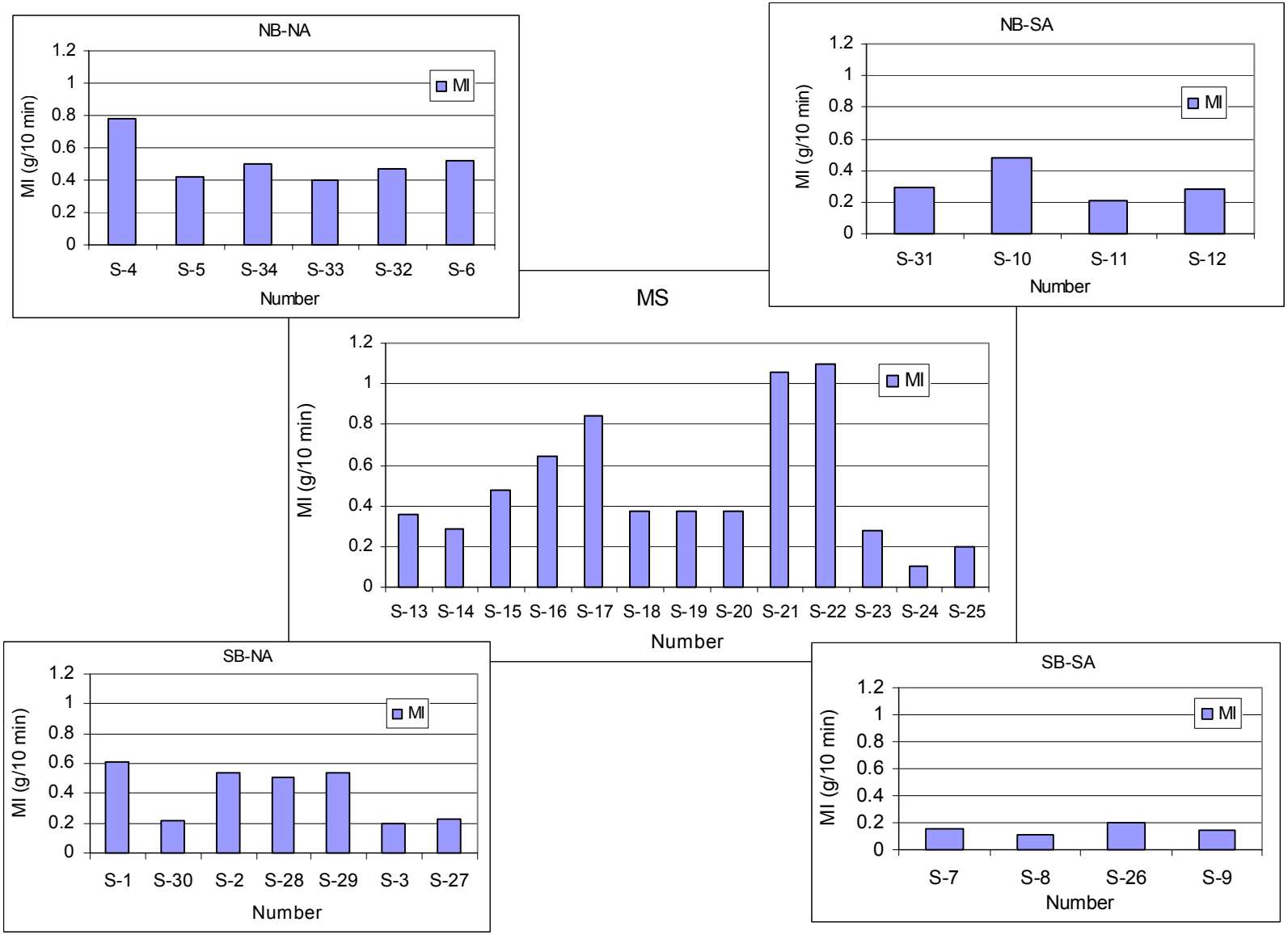

Figure 19 – MI of thirty-four span samples

Table 7 – Melt Index Values of Column Samples

No.	Sample Code	Average MI (g/10 min)
Southbound		
1	91-SB-NE-5	0.26
2	91-SB-SW-5	0.30
3	103-SB-NW-12	0.42
4	118-SB-SE-6	0.62
5	118-SB-NW-6	0.25
6	131-SB-NE-5	0.48
7	131-SB-SE-6	0.91
Northbound		
8	92-NB-NE-5	0.56
9	92-NB-SW-5	0.27
10	95-NB-SE-8	0.32
11	117-NB-SW-7	0.09
12	117-NB-NW-8	0.79
13	119-NB-NW-11	0.21
14	119-NB-SE-12	0.34

Tensile yield strength – The tensile yield strength test was performed according to ASTM D 638 Type IV. The tensile values are shown in Tables 9 and 10 for column and span samples, respectively. All field samples conformed the cell class "4" of ASTM D 3350.

Table 8 – Melt Index Values of Span Samples

No.	Sample Identification	MI (g/10 min)
Southbound-North Approach (SB-NA)		
S-1	134-SB T1-SEG7	0.61
S-30	133-SB T2-SEG7-N	0.22
S-2	126-SB T1-SEG7	0.54
S-28	121-SB T2-SEG7-N	0.51
S-29	121-SB T3-SEG7-N	0.54
S-3	117-SB T1-SEG7	0.20
S-27	117-SB T1-SEG6-N	0.23
Southbound-South Approach (SB-SA)		
S-7	105-SB T1-SEG7	0.15
S-8	96-SB T1-SEG7	0.11
S-26	95-SB T2-SEG1-N	0.20
S-9	88-SB T1-SEG7	0.16
Northbound-North Approach (NB-NA)		
S-4	134-NB T1-SEG1	0.78
S-5	126-NB T1-SEG1	0.42
S-34	124-NB T3-SEG4-N	0.50
S-33	119-NB T4-SEG1	0.40
S-32	118-NB T3-SEG6-N	0.47
S-6	117-NB T1-SEG1	0.52
Northbound-South Approach (NB-SA)		
S-31	105-NB T6-SEG1-N	0.29
S-10	105-NB T1-SEG1	0.28
S-11	96-NB T1-SEG1	0.21
S-12	88-NB T1-SEG1	0.48
Main Stay (MS)		
S-13	116-T116-W325-SEG1	0.36
S-14	115-T115-E-209-SEG19	0.29
S-15	115-T116-W-408-SEG11	0.48
S-16	113-T113-E-320-SEG17	0.64
S-17	113-T113-E-405-SEG10	0.84
S-18	112-STAY21-W-SEG21	0.37
S-19	111-T111-W-302-SEG70	0.37
S-20	110-STAY21-E-SEG21	0.37
S-21	109-T109-W-320-SEG9	1.10
S-22	187-T109-W-405-SEG18	1.10
S-23	108-T108-W-208-SEG1	0.28
S-24	107-T107-E-408-SEG10	0.10
S-25	106-T106-E325-SEG5	0.20

Table 9 – Tensile Properties of Column Samples

No.	Sample	Average Thickness (inches)	Yield Stress (psi)	Yield Elongation* (%)	Break Stress (psi)	Break Elongation (in)	Break Elongation* (%)
Southbound							
C-1	91-SB-NE-5	0.077	4192	13.6	838	3.0	263
C-2	91SB-SW-5	0.071	4312	13.3	3079	0.2	18
C-3	103SB-NW-12	0.074	4047	13.8	1256	5.0	358
C-4	118-SB-SE-6	0.074	4317	13.0	1787	5.0	357
C-5	118-SB-NW-6	0.075	3981	14.1	1242.7	5.6	429
C-6	131SB-NE-5	0.074	3990	12.9	1355	2.0	136
C-7	131-SB-SE-6	0.077	4317	13.3	2612	1.0	103
Northbound							
C-8	92NB-SW-5	0.073	4257	12.9	738	5.0	376
C-9	92NB-NE-5	0.072	4519	12.5	1863	2.0	122
C-10	95-NB-SE-8	0.076	3858	14.3	1224	8.0	608
C-11	117-NB-SW-7	0.078	3654	15.3	2540	9.0	691
C-12	117-NB-NW-8	0.069	4356	12.6	2321	7.0	542
C-13	119-NB-NW-11	0.077	3932	14.4	1109	4.0	290
C-14	119-NB-SE-12	0.076	4294	13.1	1824	5.0	371

* the value is calculated based on cross head movement and 1.3 inch gauge length

Table 10 – Tensile Properties of Span Samples

No.	Sample	Average Thickness (inches)	Yield Stress (psi)	Yield Elongation* (%)	Break Stress (psi)	Break Elongation (in)	Break Elongation* (%)
Southbound							
S-26	95SB-T2-SEG1-N	0.075	3644	14.8	3240	16	1251
S-27	117SB-T-SEG6-N	0.073	3752	14	2234	9	729
S-28	121SB-T2-SEG7-N	0.072	3898	13.5	1810	2	137
S-29	121SB-T3-SEG7-N	0.073	3814	13.9	962	8	584
S-30	133SB-T2-SEG7-N	0.074	3786	14.7	2064	10	752
Northbound							
S-31	105NB-T6-SEG1-N	0.074	3896	14.2	1754	9	659
S-32	118NB-T3-SEG6-N	0.076	3858	14.0	1709	7	568
S-33	119NB-T4-SEG1	0.073	3947	13.2	1011	7	562
S-34	124NB-T3-SEG4-N	0.073	3869	14.1	1358.0	9.7	841

- *Flexural modulus* – The flexural test was performed according to ASTM D 790, Method 1, Procedure B. Five replicates were tested for each pipe sample. The 2% modulus values are shown in Tables 11 and 12 for column and span samples, respectively. All field samples exceed the flexural modulus required range (110,000 to 160,000 psi) according to ASTM D 3350.

Table 11 - Flexural Modulus of Column Samples

No.	Sample	Average 2% Flexural Modulus (psi)
Southbound		
C-1	91-SB-NE-5	141340
C-2	91SB-SW-5	na
C-3	103SB-NW-12	142540
C-4	118-SB-SE-6	154380
C-5	118-SB-NW-6	138060
C-6	131SB-NE-5	na
C-7	131-SB-SE-6	141940
Northbound		
C-8	92NB-SW-5	na
C-9	92NB-NE-5	na
C-10	95-NB-SE-8	134380
C-11	117-NB-SW-7	121880
C-12	117-NB-NW-8	159160
C-13	119-NB-NW-11	134080
C-14	119-NB-SE-12	151280

na = not available due to insufficient material

Table 12 - Flexural Modulus of Span Samples

No.	Sample	Average 2% Flexural Modulus (psi)
Southbound		
S-26	95SB-T2-SEG1-N	129480
S-27	117SB-T-SEG6-N	123900
S-28	121SB-T2-SEG7-N	147240
S-29	121SB-T3-SEG7-N	142540
S-30	133SB-T2-SEG7-N	122500
Northbound		
S-31	105NB-T6-SEG1-N	130640
S-32	118NB-T3-SEG6-N	125280
S-33	119NB-T4-SEG1	134360
S-34	124NB-T3-SEG4-N	130000

- *SP-NCTL test* – The test was performed according to the AASHTO M294 specification, which is developed based on the ASTM D 5397-Appendix. Five replicates were tested at applied tensile stresses that were equal to the 15% of the yield strength of the material at room temperature. The notch depth is 20% of the thickness of the specimen. The failure time of each specimen was automatically recorded to the nearest 0.1 hour. All 14 column samples were tested and the average failure time values are shown in Table 13 and Figure 20. For the 34 span samples, 19 of them were tested and their results are shown in Table 14. Figure 21 shows the SP-NCTL test results together with MI value as comparison. The data reflect large variation in the stress crack resistance between retrieved field samples.

Table 13 - SP-NCTL Test Results of Column Samples

No.	Sample	Applied Stress (psi)	Average Failure Time (hr)
Southbound			
C-1	91-SB-NE-5	629	6.6
C-2	91-SB-SW-5	644	2.0
C-3	103-SB-NW-12	608	3.9
C-4	118-SB-SE-6	648	2.5
C-5	118-SB-NW-6	597	15.1
C-6	131-SB-NE-5	600	4.7
C-7	131-SB-SE-6	648	2.0
Northbound			
C-8	92-NB-NE-5	678	3.0
C-9	92-NB-SW-5	639	5.9
C-10	95-NB-SE-8	579	5.3
C-11	117-NB-SW-7	548	33.6
C-12	117-NB-NW-8	653	2.0
C-13	119-NB-NW-11	590	7.9
C-14	119-NB-SE-12	644	3.3

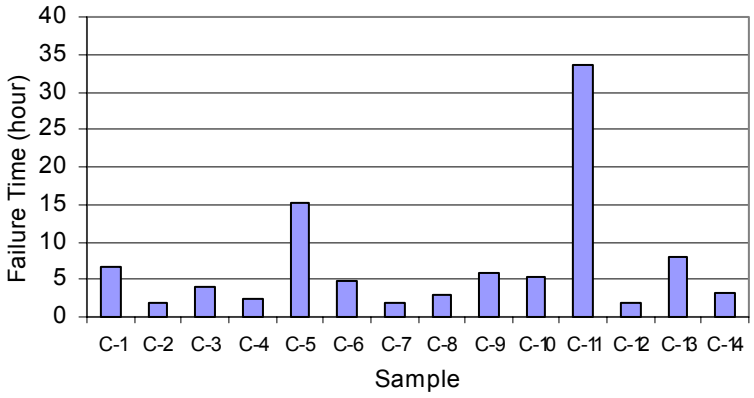

Figure 20 – Failure time of fourteen column samples

Table 14 - SP-NCTL test Results of Span Samples

No.	Sample Identification	Applied Stress (psi)	Failure Time (hr)
Southbound-North Approach (SB-NA)			
S-30	133-SB T2-SEG7-N	568	3.4
S-2	126-SB T1-SEG7	675	3.5
S-28	121-SB T2-SEG7-N	579	2.6
S-29	121-SB T3-SEG7-N	572	4.5
S-27	117-SB T1-SEG6-N	563	8.6
Southbound-South Approach (SB-SA)			
S-8	96-SB T1-SEG7	685	7.5
S-26	95-SB T2-SEG1-N	547	7.7
S-9	88-SB T1-SEG7	675	8.0
Northbound-North Approach (NB-NA)			
S-5	126-NB T1-SEG1	664	4.0
S-34	124-NB T3-SEG4-N	580	3.6
S-33	119-NB T4-SEG1	592	6.7
S-32	118-NB T3-SEG6-N	579	3.1
Northbound-South Approach (NB-SA)			
S-31	105-NB T6-SEG1-N	584	9.3
S-10	105-NB T1-SEG1	676	5.7
S-12	88-NB T1-SEG1	710	3.0
Main Stay (MS)			
S-16	113-T113-E-320-SEG17	662	3.6
S-17	113-T113-E-405-SEG10	657	2.8
S-19	111-T111-W-302-SEG70	669	11.5
S-21	109-T109-W-320-SEG9	667	3.1

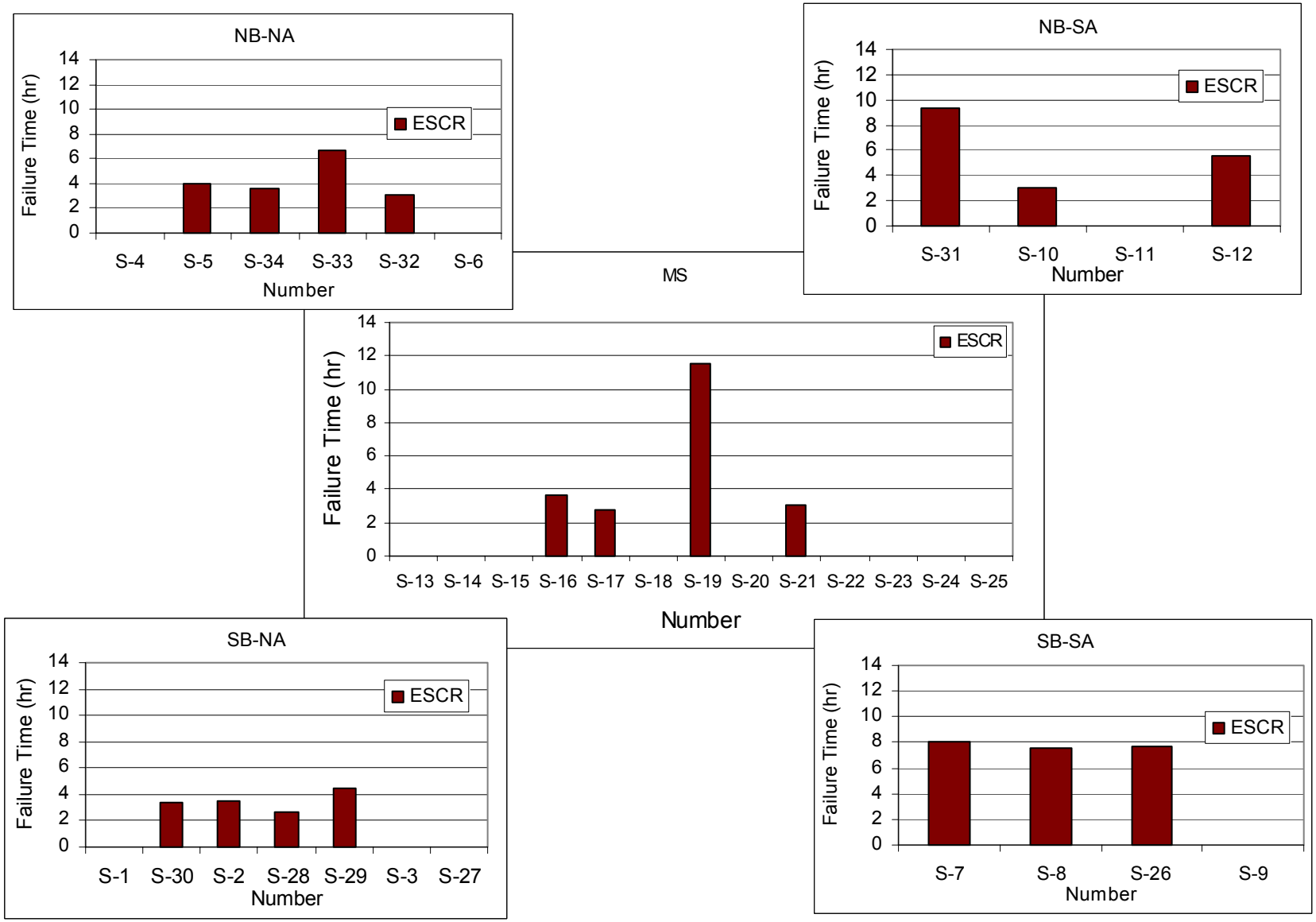

Figure 21 – Failure time of eighteen span samples

OIT test – The test was performed according to ASTM D3895. The test is used to assess the time required to oxidize the test specimen at an isothermal temperature of 200°C. Two replicates were tested for majority of the samples. Test specimens were taken directly from duct samples. The average OIT values of column and span samples are shown in Tables 15 and 16, respectively. The bar chart plots are shown in Figures 22 and 23 for column and span samples, respectively. The OIT values of all field samples are less than 10 minutes. Many of the span samples exhibited OIT value of approximately 2 minutes.

Table 15 - OIT Values of Column Samples

No.	Sample Code	Average OIT (min)
Southbound		
C-1	91-SB-NE-5	5.0
C-2	91-SB-SW-5	4.4
C-3	103-SB-NW-12	2.7
C-4	118-SB-SE-6	3.2
C-5	118-SB-NW-6	4.6
C-6	131-SB-NE-5	4.4
C-7	131-SB-SE-6	2.9
Northbound		
C-8	92-NB-NE-5	4.3
C-9	92-NB-SW-5	6.5
C-10	95-NB-SE-8	3.9
C-11	117-NB-SW-7	6.8
C-12	117-NB-NW-8	2.3
C-13	119-NB-NW-11	8.1
C-14	119-NB-SE-12	5.9

Table 16 - OIT Values of Span Samples

No.	Sample Code	Average OIT (min)
Southbound		
S-26	95SB-T2-SEG1-N	6.5
S-27	117SB-T1-SEG6-N	8.4
S-28	121SB-T2-SEG7-N	2.4
S-29	121SB-T3-SEG7-N	2.0
S-30	133SB-T2-SEG7-N	5.8
Northbound		
S-31	105NB-T6-SEG1-N	1.9
S-32	118NB-T3-SEG6-N	2.5
S-33	119NB-T4-SEG1	2.4
S-34	124NB-T3-SEG4-N	2.8

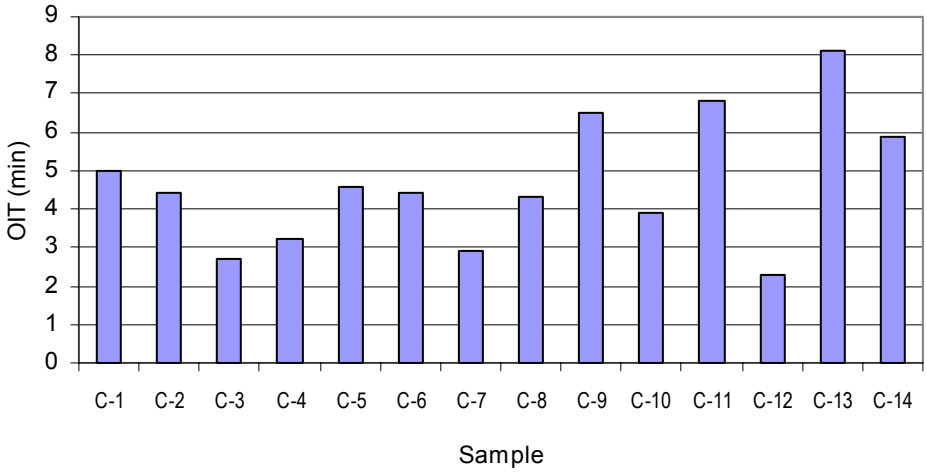

Figure 22 – OIT values of column samples

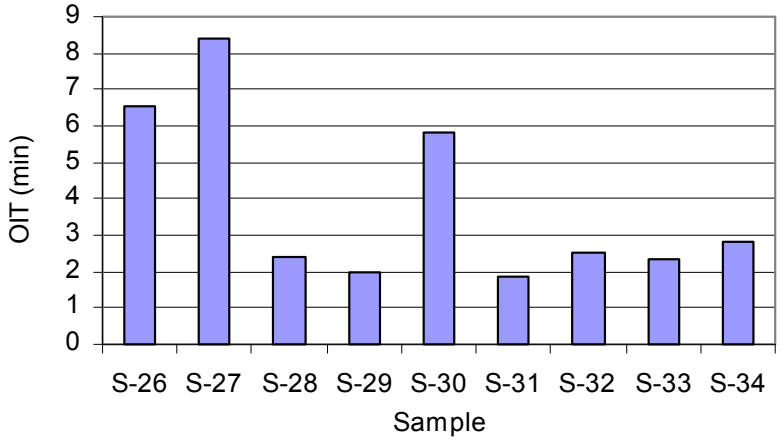

Figure 23 – OIT values of span samples

Discussion of Material Properties

It is well known that the SCR of HDPE is related to the molecular weight and crystallinity of the material as well as other factors such as polymerization techniques, type of catalysts and co-monomers. In this study, the molecular weight of polymer is assessed using the MI test, the crystallinity is reflected by the density, and SCR is measured by the failure time of the SP-NCTL test. The cracked duct samples exhibited higher MI and density values than non-cracked ducts. (A high MI indicates a low molecular weight, while high density signifies high crystallinity.) Both high MI and density have negative impact on the SCR of the material. However, the MI test has a greater accuracy than the density test.

Figure 24 shows the graph plotting MI value against failure time of the SP-NCTL test for all tested field samples, except one data with failure time over 30 hours. The data can be divided into two groups according to different MI ranges, as follows:

- MI value greater than 0.4 g/10 min, the failure time less than 5 hours
- MI value less than 0.4 g/10 min, failure time ranges from 2 to 34 hours.

Clearly, samples with MI values greater than 0.4 g/10 min are highly susceptible to stress cracking. Six out of 14 column samples and 15 out of 34 span samples have MI values greater than 0.4 g/10 min. For samples with MI values less than 0.4 g/10 min, the majority of them have failure times longer than 5 hours.

In order to identify the cracking potential of the ducts in different sections of the bridge, the MI and SP-NCTL failure time are placed side-by-side for each section, as shown in Figure 25 (a) to (e). Ducts in the SB-SA section have the lowest MI values and consistent failure times of 8 hours. In addition, ducts in the center stay (S-18, S-19 and S-20) exhibited the highest SCR property, while ducts with the worst SCR are located on both sides of the center stay.

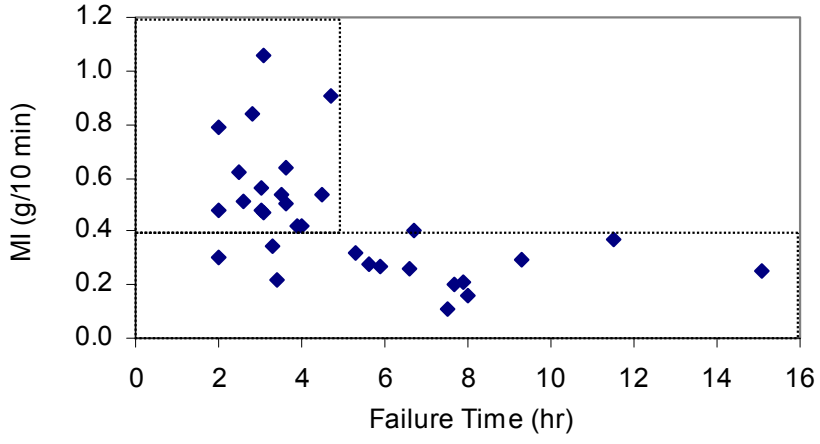

Figure 24 – Failure Time versus MI of all evaluated field samples

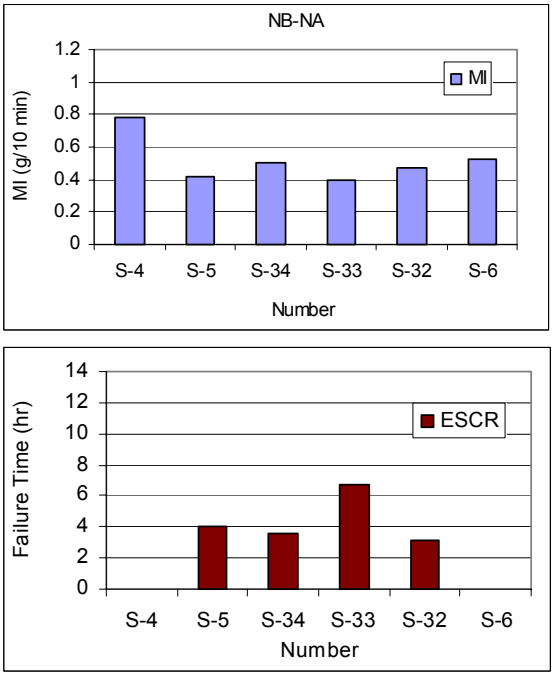
NB-NA
MI (g/10 min)
1.2
1
0.8
0.6
0.4
0.2
0
MI
S-4
S-5
S-34
S-33
S-32
S-6
Number
Failure Time (hr)
14
12
10
8
6
4
2
0
ESCR
S-4
S-5
S-34
S-33
S-32
S-6
Number

(a)

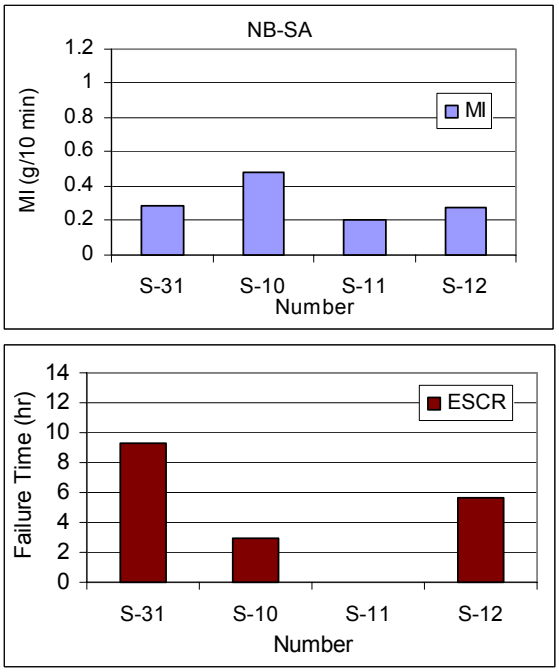
NB-SA
MI (g/10 min)
1.2
1
0.8
0.6
0.4
0.2
0
MI
S-31
S-10
S-11
S-12
Number
Failure Time (hr)
14
12
10
8
6
4
2
0
ESCR
S-31
S-10
S-11
S-12
Number

(b)

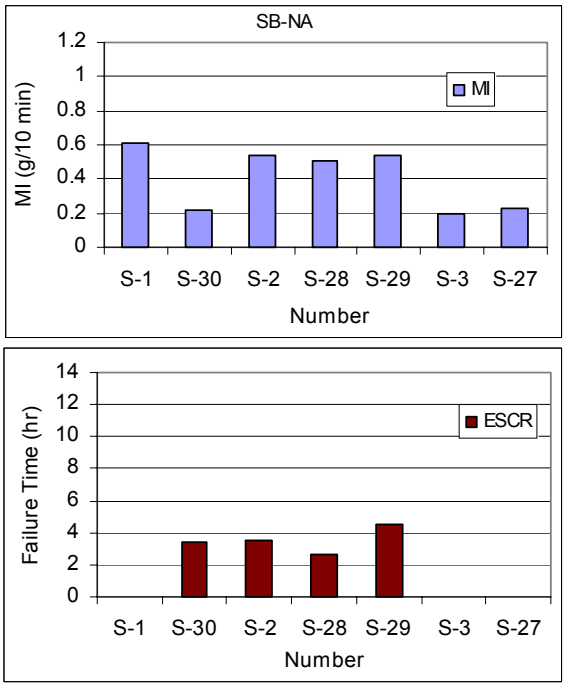
SB-NA
MI (g/10 min)
1.2
1
0.8
0.6
0.4
0.2
0
MI
S-1
S-30
S-2
S-28
S-29
S-3
S-27
Number
Failure Time (hr)
14
12
10
8
6
4
2
0
ESCR
S-1
S-30
S-2
S-28
S-29
S-3
S-27
Number

(c)

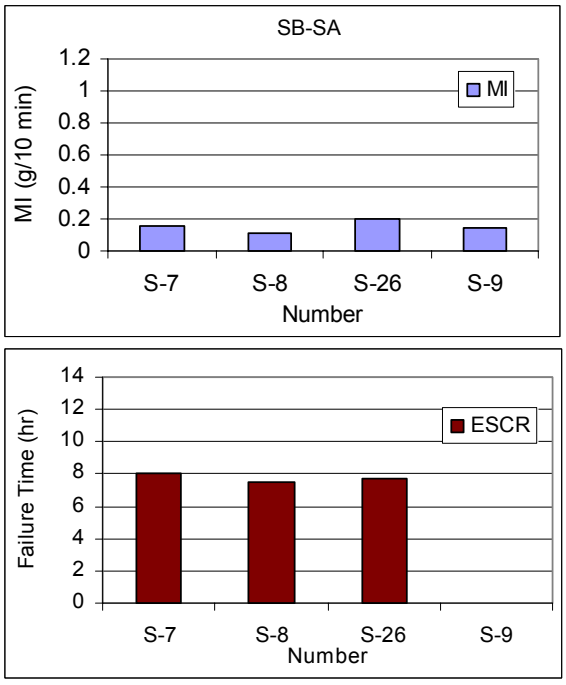
SB-SA
MI (g/10 min)
1.2
1
0.8
0.6
0.4
0.2
0
MI
S-7
S-8
S-26
S-9
Number
Failure Time (hr)
14
12
10
8
6
4
2
0
ESCR
S-7
S-8
S-26
S-9
Number

(d)

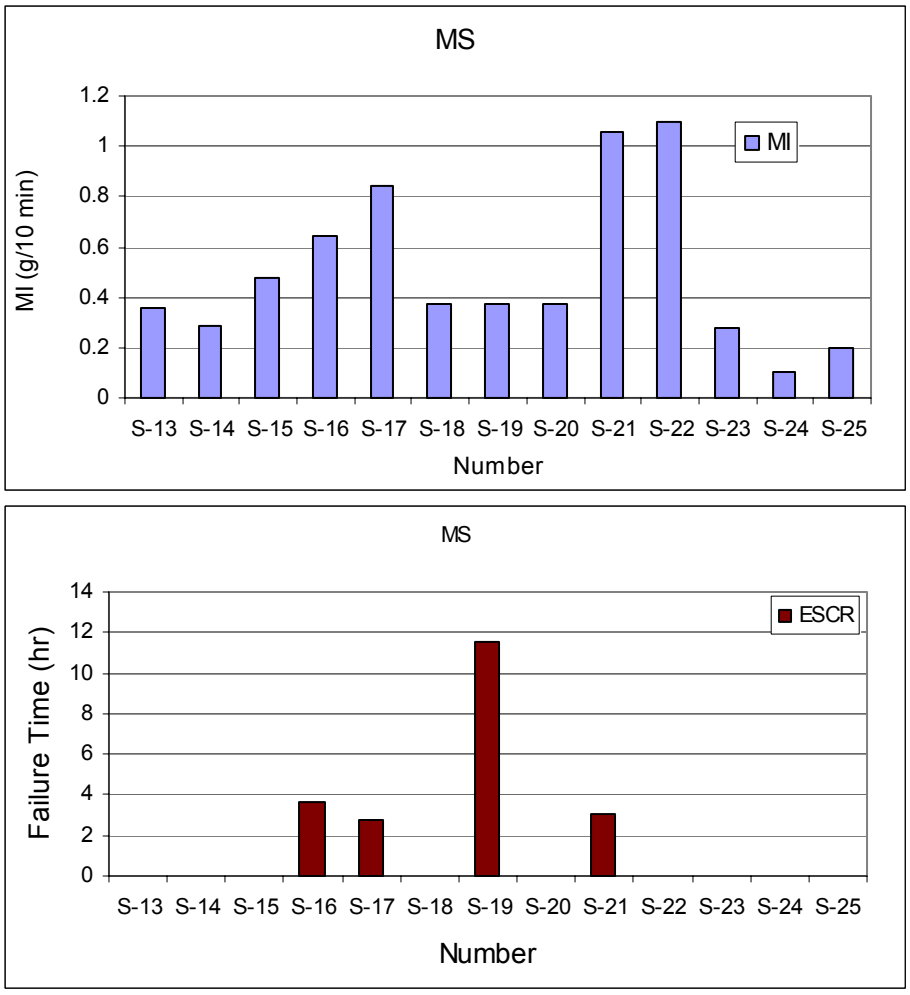

(e)

Figure 25 – Comparing MI and failure time of span samples

Figure 26 shows the graph plotting density against failure time. It seems that the correlation between density and failure time is very poor. Nevertheless, samples with high density values tend to have short failure times. Samples with density less than 0.948 g/cc have failure times greater than 5 hours.

In summary, molecular weight (MI) and crystallinity (density) can have effected on the SCR, but they cannot confidently predict the SCR of the material. Samples with low MI and density in general exhibit higher SCR as reflected by the long failure time in the SP-NCTL test. Between MI and density properties, the MI correlates to SCR slightly better than density.

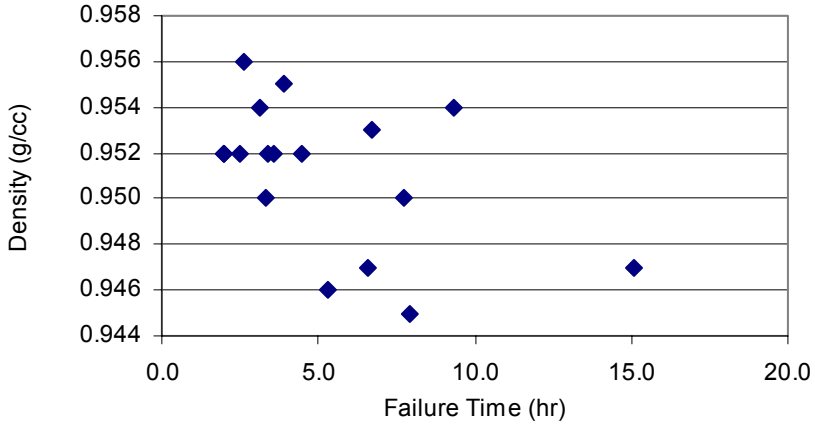

Figure 26 – Density versus failure time of all evaluated field samples

CONCLUSIONS

Duct samples were retrieved from both the column and superstructure of the SSK Bridge. Fourteen samples were taken from various columns of which four contained a longitudinal crack. From the superstructure, 34 samples were removed and three of the samples had longitudinal cracks. The cracking mechanisms were investigated on two samples, one from the column (131-SB-SE-6) and one from the superstructure (Span 124NB-T3-SEG4-N). The fracture morphology indicated that the slow crack growth was the governing mechanism. The crack initiations of column samples were caused by defects in the inner surface of the duct. For the span sample, the crack initiation could not be identified on the section of the cracked duct evaluated. However, impurities were observed in the examined sample. In addition, fatigue lines were observed on the fracture surface indicating that a cycling loading involved in the crack growth.

The material properties were evaluated according to AASHTO specification based on ASTM D 3350 material specification. Two of the specified tests were not performed due to sample configuration and poor precision of the test. However, SP-NCTL test and OIT test are added to the material evaluation. In Table 17, resulted test values are compared with corresponding specified values that were defined by the AASHTO specification. The majority of the field samples failed to conform melt index and carbon black requirements. For SP-NCTL test, except for two column samples, all other samples exhibited failure times less than 10 hours. Regarding the long-term stability of the duct, the OIT test was used to assess the amount of antioxidant remaining in the ducts. All field samples have OIT values less than 10 minutes. The four span samples taken from the Northbound had OIT value less than 3 minutes. Although the OIT values were very low, some antioxidants still remained in the duct to protect the

mechanical properties. For the SSK Bridge, it would be important to monitor the depletion of antioxidants with time, particularly for ducts along the northbound of the spans.

Table 17 – Comparing Test Results with Specified Values

Property	ASTM D 3350 Classification	Required Value	Test Results
Density (g/cc)	3	>0.940-0.955	0.945 – 0.956
Melt Index (g/10 min)	4	< 0.15	0.09 – 0.91
Flexural Modulus (psi)	5	110,000 - < 160,000	124,000 – 159,000
Tensile Strength (psi)	4	3000 -<3500	3600 - 4500
Carbon black (%)	C	> 2	0.20 – 1.7
Additional Tests			
SP-NCTL (hour)		> 24	2.0 – 33.6
OIT (min)		Not defined	1.9 – 8.4

Based on test data of fourteen duct samples that were taken from different columns of the SSK Bridge, the quality of the ducts varies significantly. The wall thickness variability is outside the specification requirement. The MI and density test data suggest that these ducts were not manufactured from the same lot of resin. The large different in the MI values, from 0.09 to 0.9 g/cc, may even imply that these ducts were fabricated from different extrusion processes.

The test results also indicate large variability in the properties of 34 retrieved span samples. The greatest variability is observed in the main stay section of the bridge. In the four approaching sections, ducts taken from SB-SA have the most uniform material properties. In addition, there seems to be two groups of resins, one with MI around 0.25 g/10 min and the other around 0.48 g/10 min.

By comparing failure time of the SP-NCTL tests to density and MI, the relatively low molecular weight (high MI) and high crystallinity (high density) of the resins are contributing factors to the cracking.